

1 **Characterization of water-soluble brown carbon chromophores**
2 **from wildfire plumes in the western US using size exclusion**
3 **chromatography**

4 Lisa Azzarello¹, Rebecca A. Washenfelder², Michael A. Robinson^{2,3}, Alessandro Franchin^{2,3,4},
5 Caroline C. Womack^{2,3}, Christopher D. Holmes⁵ Steven S. Brown^{2,6}, Ann Middlebrook², Tim
6 Newberger⁷, Colm Sweeney⁷, Cora J. Young¹

7 ¹Department of Chemistry, York University, Toronto, ON, M3J 1P3, Canada

8 ²Chemical Sciences Laboratory, National Oceanic and Atmospheric Administration, 325
9 Broadway, Boulder, CO 80305, USA

10 ³Cooperative Institute for Research in Environmental Sciences (CIRES), University of Colorado,
11 Boulder, CO, 80309, USA

12 ⁴Now at: National Center for Atmospheric Research, Boulder, CO, USA

13 ⁵Earth, Ocean, and Atmospheric Science, Florida State University, Tallahassee, FL 32304, USA

14 ⁶Department of Chemistry, University of Colorado Boulder, Boulder, Colorado, USA

15 ⁷Global Monitoring Laboratory, National Oceanic and Atmospheric Administration, 325
16 Broadway, Boulder, CO 80305, USA

Correspondence to: C. J. Young (youngcj@yorku.ca)

17 **Abstract**

18 Wildfires are an important source of carbonaceous aerosol in the atmosphere. Organic
19 aerosol that absorbs light in the ultraviolet to visible spectral range is referred to as “brown carbon”
20 (BrC), and its impact on Earth’s radiative budget has not been well characterized. We collected
21 water-soluble brown carbon using a particle into liquid sampler (PILS) onboard a Twin Otter
22 aircraft during the Fire Influence on Regional to Global Environments and Air Quality (FIREX-
23 AQ) campaign. Samples were collected downwind of wildfires in the western United States from
24 August to September 2019. We applied size exclusion chromatography (SEC) with ultraviolet-
25 visible spectroscopy to characterize the molecular size distribution of BrC chromophores. The
26 wildfire plumes had transport ages of 0 to 5 h and the absorption was dominated by chromophores
27 with molecular weights <500 Da. With BrC normalized to a conserved biomass burning tracer,
28 carbon monoxide, a consistent decrease in BrC absorption with plume age was not observed during
29 FIREX-AQ. These findings are consistent with the variable trends in BrC absorption with plume
30 age reported in recent studies. While BrC absorption trends were broadly consistent between the
31 offline SEC analysis and the online PILS measurements, the absolute values of absorption and
32 their spectral dependence differed. ~~We attribute this difference to the organic modifier used in the
33 chromatographic separation and demonstrate how this affects the molecular structure of the
34 compounds comprising BrC, with implications for interpretation of absorption measurement of
35 BrC field samples.~~We investigate plausible explanations for the discrepancies observed between
36 the online and offline analyses. This included solvent effects, pH, and sample storage. We suspect
37 that sample storage impacted the absorption intensity of the offline measurements without
38 impacting the molecular weight distribution of BrC chromophores.

39 **1. Introduction**

40 The wildfire season across the western United States has greatly intensified over the past
41 century. The U.S. Forest Service reports that the amount of western U.S. land burned by “high
42 severity” wildfires (i.e., fires that destroy more than 95% of vegetation) has increased eightfold
43 since 1985 (Parks and Abatzoglou, 2020). A variety of factors influence the number and intensity
44 of wildfires, including fuel availability, temperature, drought conditions, location of lightning
45 strikes, and direct human influence. During the 20th century, fire suppression tactics were applied
46 throughout the western U.S. and these efforts caused fuel to accumulate (Marlon et al., 2012). The
47 combination of dry conditions, warmer temperatures, and fuel availability contributes to the
48 intensity of present-day wildfires in the western U.S. Consequently, the impact that these climatic
49 conditions have on wildfire activity has been established. However, feedback effects that wildfires
50 have on climate is an ongoing area of research.

51 Wildfires emit carbonaceous particulate matter into the atmosphere (Bond et al., 2004; van
52 der Werf et al., 2010). Based on volatility and optical properties, carbonaceous aerosol particles
53 emitted from biomass burning are categorized as elemental carbon (EC) and organic carbon (OC)
54 (Turpin et al., 1990). Elemental carbon, referred to as black carbon (BC), is refractory and is
55 characterized by broad absorbance across the ultraviolet (UV) to infrared wavelengths (Seinfeld
56 and Pankow, 2003; Andreae and Gelencsér, 2006; Laskin et al., 2015). The light-absorbing
57 components of organic aerosols are referred to as brown carbon (BrC) (Laskin et al., 2015). The
58 direct absorption and scattering of solar radiation by these aerosol particles impacts the global
59 radiative budget (Boucher, O.; Randall, D.; Artaxo, P.; Bretherton, C.; Feingold et al., 2013;
60 Forster, P.; Ramaswamy, V.; Artaxo, P.; Berntsen, T.; Betts et al., 2007), but there is uncertainty
61 about the magnitude of this effect. ~~Currently, more information is known about BC and its impact~~
62 ~~on climate than BrC, as BrC is more chemically complex and more reactive (Buis, 2021; Di~~
63 ~~Lorenzo et al., 2017)~~Currently, more information is known about BC and its impact on climate
64 than BrC, as BrC is more chemically complex and more reactive (Buis, 2021; Di Lorenzo et al.,
65 2017). The direct radiative forcing of BC has been estimated to be the second largest anthropogenic

66 climate forcing species (Ramanathan and Carmichael, 2008) and studies have suggested that BrC
67 can contribute between 20 to 40 % to positive radiative forcing from total carbonaceous absorbing
68 aerosol (Feng et al., 2013; Zhang et al., 2017; Zeng et al., 2020a).

69 Wildfire emissions are a dominant primary source of BrC (Washenfeller et al., 2015). The
70 brown colour results from a combination of species with varying abilities to absorb light in the
71 UV-visible region (from highly to weakly absorbing) (Hems et al., 2021). The pyrolysis of lignin
72 and cellulose contributes to the major chemical constituents in wildfire plumes, such as phenolic
73 compounds and organic acids (Simoneit, 2002; Xie et al., 2019; Smith et al., 2014). Lignin
74 pyrolysis products with aromatic functionalities absorb visible light and may contribute to the
75 absorption properties of BrC (Hems et al., 2021). Secondary processes also contribute to BrC
76 formation. The generation of secondary organic aerosol (SOA) stemming from gas phase reaction
77 products includes nitration of aromatic compounds in the presence of NO_x or NO₃ (Harrison et al.,
78 2005; Finewax et al., 2018; Xie et al., 2017). For example, catechol can react with either the NO₃
79 or OH radical to form 4-nitrocatechol (Finewax et al., 2018) and oxidation of toluene under
80 elevated NO_x conditions has been observed to form over 15 absorbing compounds with
81 nitroaromatics contributing up to 60% of absorption in the visible region (Liu et al., 2016).
82 Although there are hypotheses about the identity of BrC chromophores, up to 40% of BrC
83 constituents remain unidentified (Lin et al., 2017; Bluvshstein et al., 2017).

84 To characterize the absorbing constituents that contribute to BrC absorption, reverse phase
85 high performance liquid chromatography (HPLC) coupled to high resolution mass spectrometry
86 has been applied (Fleming et al., 2020). However, fresh and aged BrC consist of extremely low
87 volatile organic compounds (ELVOCs) that may be irreversibly retained on a traditional C₁₈
88 reverse phase HPLC column (Di Lorenzo and Young, 2016). Size exclusion chromatography
89 coupled to ultraviolet-visible absorption spectroscopy (SEC-UV) has been demonstrated as an
90 alternative that successfully measures the absorption properties of high and low molecular weight
91 (MW) ELVOCs in fresh and aged biomass burning-derived samples (Di Lorenzo and Young,
92 2016; Di Lorenzo et al., 2017; Wong et al., 2019). Analysis by SEC-UV has been previously
93 applied to samples collected during ground-based field measurement campaigns, where the
94 method has established the quantification of BrC absorbance as a function of MW and provided
95 insight into the composition of BrC. High MW (>400 Da) compounds with unknown structural
96 identities have been determined to contribute to BrC absorption and the relative contribution to

97 BrC absorption by high MW species increases with smoke age (Di Lorenzo et al., 2017; Wong et
98 al., 2017, 2019). These findings suggested that lower MW species are less- persistent in biomass
99 burning smoke relative to higher MW species, likely due to volatilization, oxidation,
100 polymerization, or other processes (Di Lorenzo et al., 2017; Hems et al., 2021).

101 The Fire Influence on Regional to Global Environments and Air Quality (FIREX-AQ) field
102 campaign examined the impact of wildfires on atmospheric chemistry and air quality in the western
103 United States. In this work, we present the SEC-UV analysis of water-soluble BrC that was
104 collected on board the National Oceanic and Atmospheric Administration (NOAA) Twin Otter
105 aircraft during plume transects downwind from western U.S forest fires. These represent the first
106 aircraft samples analyzed by SEC-UV to characterize BrC. We compare the total absorption
107 measured in online and offline samples and [attribute](#)-assign the BrC absorption to different MW
108 classes. Finally, we examine how the composition of the mobile phase used in the SEC-UV
109 analysis impacts elution time and spectral features. This provides cautionary information about
110 interpreting absorption results in studies that apply chromatographic separation in an aqueous-
111 organic matrix.

112

113 **2. Experimental Approach**

114 **2.1 Overview of the FIREX-AQ field campaign**

115 FIREX-AQ was a multi-platform field campaign that investigated wildfire emissions in the
116 western United States from Jul to Sep 2019. Instrumented aircraft and mobile laboratories were
117 used to intercept and sample smoke plumes throughout multiple western U.S. states. These
118 included a DC-8, ER-2, and two Twin Otter aircraft. This study focuses on smoke sampled by the
119 “Chemistry” Twin Otter aircraft, which was based in Boise, Idaho, from 29 Jul to 5 Sep 2019, and
120 briefly in Cedar City, Utah, from 19 Aug to 23 Aug 2019. The Twin Otter payload included gas
121 and aerosol instruments to measure smoke composition, transport, and transformation. This
122 included CO measurements by near infrared cavity ring-down spectroscopy ([G2401-m](#); Picarro
123 [G2401mInc., Santa Clara, CA, USA](#)) (Crosson, 2008; Karion et al., 2013). A complete description
124 of the payload installed on the Twin Otter can be found in Warneke et al. (2023). The payload
125 [weight](#) limited the duration of in-flight sampling to 2.5 – 3 h, with a typical schedule of two or
126 three flights per day during the afternoon, evening, or night. A total of 40 flights were completed
127 in Arizona, Idaho, Nevada, Oregon, and Utah. Airmass back trajectory analyses were used to

128 estimate the plume age of each transect, as described in Liao et al. (2021) and Washenfelder et al.
129 (2022). Briefly, the smoke age was calculated by summing the horizontal advection and vertical
130 plume rise ages between the time of emission and the aircraft interception of the smoke plume.
131 For the Twin Otter flights, many plume intercepts by the aircraft were approximately Lagrangian
132 (Washenfelder et al., 2022).

133 **2.2 Online measurement of water-soluble absorption and offline sample collection**

134 The Brown Carbon-Particle into Liquid Sampler (BrC-PILS) collected online absorption
135 data and offline aqueous samples for the SEC-UV analysis. A complete description of the BrC-
136 PILS instrument and sampling can be found in Zeng et al. (2021) and Washenfelder et al. (2022).
137 Briefly, the BrC-PILS sampled smoke through a shared aerosol inlet on the Twin Otter. A parallel-
138 plate carbon filter denuder removed volatile organic compounds prior to the aerosol entering the
139 PILS. The PILS consisted of a steam generator and droplet impactor to collect aerosols into
140 aqueous solution. The liquid flow then entered a liquid waveguide capillary cell (LWCC) to
141 measure absorption. The instrument precision (3σ) for absorption at 365 nm was $\pm 0.02 \text{ Mm}^{-1}$
142 for 10 s in-flight data, with an uncertainty of $\pm 11\%$ (Zeng et al., 2021). The flow exiting the
143 LWCC was split between a total organic carbon (TOC) analyzer and an automated 14-port valve.
144 The valve directed aqueous sample flow to one of 12 polypropylene sample tubes for offline SEC-
145 UV analysis (Figure S1). Prior to deployment, each polypropylene tube was rinsed with 18.2
146 $\text{M}\Omega\cdot\text{cm}$ [deionized water \(DIW\)](#) (Thermo Scientific Barnstead Smart2Pure) eight to ten times. The
147 sample flow rate was monitored by a liquid mass flow meter prior to the flow diverting between
148 the automated valve and the TOC analyzer. The sample flow was 1.53 mL min^{-1} during inflight
149 sampling, and the excess 0.43 mL min^{-1} was collected into an individual polypropylene tube for
150 12 s to 10 min. During in-flight sampling, the flight scientist actively controlled the sample
151 collection into each polypropylene tube to target transects of the smoke plume (example shown in
152 Figure S2). Six to twelve aqueous samples were collected for each flight, with 201 total samples
153 from 39 science flights. Field blanks of the [18.2 \$\text{M}\Omega\cdot\text{cm}\$ water \(DIW\)](#) used to operate the BrC-
154 PILS were stored similarly in clean polypropylene sample tubes at the beginning, halfway point,
155 and end of campaign. Once collected in the field, the samples and blanks were stored on ice for
156 several hours prior to refrigeration until analysis.

157

158 **2.3 Offline Analysis by SEC-UV**

159 Measurement by SEC-UV provides information about size-dependent light absorption
160 properties of BrC chromophores. The offline aerosol samples were separated using an aqueous
161 gel-filtration column with a MW range of 250 Da to 75 kDa (Polysep GFC P-3000, Phenomenex,
162 Torrence, CA). Size-resolved components were detected using a diode array detector from 190 to
163 800 nm (UltiMate 3000, Thermo Scientific, Sunnyvale, CA) coupled to an ion chromatograph
164 (ICS 6000; Thermo Scientific) pump with an AS autosampler (Thermo Scientific). The isocratic
165 method was run using a [mobile phase that contained a 1:1 mixture of acetonitrile and a buffer](#)
166 [solution consisting of 18.2 MΩ-cm deionized water with 25 mM ammonium acetate in solution](#) at
167 a flow rate of 1 mL min⁻¹ and a sample injection volume of 100 μL. [A solution of Suwannee River](#)
168 [Humic Acid \(SRHA II, International Humic Substances Society, Saint Paul, MN, USA\)](#) was run
169 [prior to the FIREX-AQ samples to ensure proper operation of the SEC-UV set-up.](#)

170 [The aqueous samples collected by the BrC-PILS did not require post-sampling processing](#)
171 [and were injected onto the SEC column under mobile phase flow to the diode array detector. The](#)
172 [uncertainty for the offline total absorption measurements considers the uncertainty of the liquid](#)
173 [flow and PILS collection efficiency, for a total uncertainty of ±10.5 %.](#) Discussion of the SEC-UV
174 method development and details of the conversion of SEC-UV signal to ambient absorption in
175 units of Mm⁻¹ can be found in the SI. We calculated BrC absorption as a function of MW by
176 applying the calibration method described by Di Lorenzo and Young (2016) (Figure S3). Sample
177 measurements were blank subtracted. The detection limit of the total integrated absorption
178 (equivalent to 3σ of n=6 field blanks) was 2.5±0.2 mAU×min and 0.70±0.02 mAU×min at 250 nm
179 and 300 nm, respectively. This corresponds to [a 3σ detection limit of](#) approximately 525 Mm⁻¹ at
180 250 nm and 150 Mm⁻¹ at 300 nm.

181

182 [2.4 Absorption in different mobile phases](#)

183 [To assess the impact of pH and mobile-phase composition on wavelength-dependent](#)
184 [absorption, the ammonium acetate solution was adjusted to pH 5 and pH 9 with acetic acid and](#)
185 [ammonium hydroxide, respectively, prior to combining with acetonitrile. A 15 μg/mL in DIW](#)
186 [solution of Suwannee River Fulvic Acid \(SRFA II; International Humic Substances Society, Saint](#)
187 [Paul, MN, USA\) and a FIREX-AQ aqueous sample were injected onto the diode array detector](#)
188 [without the SEC column in line with the following mobile phases: DIW only; 25 mM ammonium](#)
189 [acetate solution; the default mobile phase \(described in Sect. 2.3\); 25 mM ammonium acetate](#)

190 [solution adjusted to pH 5; and 25 mM ammonium acetate solution adjusted to pH 9. Solutions of](#)
191 [4-nitrocatechol, 4-hydroxy-3-methoxy cinnamaldehyde, vanillin, and 7-hydroxycoumarin in DIW](#)
192 [with concentrations of \$3.9 \times 10^{-8}\$, \$3.4 \times 10^{-8}\$, \$3.9 \times 10^{-8}\$, \$3.7 \times 10^{-8}\$ mol/mL, respectively, were prepared](#)
193 [and injected onto the diode array detector to observe differences in their absorption profiles. To](#)
194 [confirm the diode array detector results, measurements of the SRFA solution were also made with](#)
195 [UV-visible spectroscopy \(8453; Agilent Technologies, Santa Clara, CA, USA\) where the solution](#)
196 [was mixed \(1:1 ratio\) with the various mobile phases prior to transferring to a cuvette for](#)
197 [absorption measurements \(Figure S7\).](#)

198 3. Results and discussion

199 3.1. Trends in absorption with plume age

200 We present molecular size-resolved absorption for flights that met the following criteria:
201 (1) maximum CO concentrations greater than 0.2 ppmv; (2) three or more downwind plume
202 transects; (3) three or more aqueous samples collected; and (4) consistent wind direction. Of the
203 201 aqueous samples collected, 47 samples from six flights met the criteria and are summarized
204 in Table S1. Each aqueous sample had a measurable absorption signal in the deep UV region (250
205 to 300 nm), while the absorption signal above 300 nm was nearly indistinguishable from the
206 blanks, because the samples were relatively dilute. The average (\pm standard deviation) integrated
207 absorption of the 47 samples that met the criteria was 10.4 ± 4.9 mAU \times min (8134 ± 3857 Mm $^{-1}$) and
208 0.36 ± 0.28 mAU \times min (316 ± 214 Mm $^{-1}$) for 250 and 300 nm, respectively.

209 To account for plume dilution, we follow the convention of normalizing BrC absorption to
210 a conserved tracer, to calculate $\Delta \text{Abs}_{\lambda, \text{BrC}} / \Delta \text{CO}$ (~~Forrister et al., 2015; Di Lorenzo et al., 2017;~~
211 ~~Washenfelder et al., 2022; Zeng et al., 2021~~)(Forrister et al., 2015; Di Lorenzo et al., 2017;
212 ~~Washenfelder et al., 2022; Zeng et al., 2021; Sullivan et al., 2022~~), where ΔCO is the average CO
213 mixing ratio measured during each aqueous sample collection subtracted ~~from~~by the average CO
214 background outside the plume. -Background BrC absorption at 365 nm (a common wavelength to
215 report BrC absorption) was less than 0.2 Mm $^{-1}$ and no background correction was made to
216 determine $\Delta \text{Abs}_{\lambda, \text{BrC}}$ (Washenfelder et al., 2022). [The average CO and variation of CO measured](#)
217 [for each flight are shown in Figure S9.](#) Figure 1 shows $\Delta \text{Abs}_{300\text{nm}, \text{BrC}} / \Delta \text{CO}$ as a function of plume
218 age for the six selected flights, with a linear fit to each flight. The fitted slopes for $\Delta \text{Abs}_{300\text{nm},$
219 $\text{BrC} / \Delta \text{CO}$ vs plume age vary from -0.21 to 0.88 Mm $^{-1}$ ppbv $^{-1}$ h $^{-1}$, and show different trends between

220 flights. This indicates that BrC absorption increased downwind in some plumes and decreased
221 downwind in others.

222 Previous studies of normalized BrC absorption with plume age have reported conflicting
223 results. In the earliest aircraft study, Forrister et al. (2015) collected filter samples from two fires
224 in the western U.S. and measured the BrC absorption from water and methanol extracts. They
225 observed that BrC absorption at 365 nm decayed exponentially over a plume age range spanning
226 0 to 50 h (Figure S6S10) (Forrister et al., 2015). Di Lorenzo et al. (2017) reported total absorption
227 of size-resolved BrC chromophores using SEC-UV from three locations that were influenced to
228 varying degrees by biomass burning smoke, and observed minimal $\Delta\text{Abs}_{\lambda, \text{BrC}}/\Delta\text{CO}$ change as a
229 function of transport times from 10 to >72 h (Figure S6S10). In contrast to these measurements of
230 relatively aged biomass burning aerosol, two studies from other FIREX-AQ instruments showed
231 different trends for relatively fresh plumes. Using BrC-PILS measurements from the Twin Otter,
232 Washenfelder et al. (2022) showed variable trends in $\Delta\text{Abs}_{365\text{nm}, \text{BrC}}/\Delta\text{CO}$ slope values ranging
233 from -0.02 to 0.02 $\text{Mm}^{-1} \text{ppbv}^{-1} \text{h}^{-1}$ over 0 to 5 h. Using filter samples from the DC-8 aircraft, (Zeng
234 et al., 2022) showed that BrC increased, decreased, or was unchanged as a function of plume
235 age over 0 to 8 h. In another study of fresh plumes, aircraft based measurements during the
236 Western Wildfire Experiment for Cloud Chemistry, Aerosol Absorption and Nitrogen (WE-CAN;
237 Sullivan et al., 2022) investigated the evolution of water-soluble BrC at 405 nm normalized to CO
238 and observed BrC depletion with a smoke age of <2 h, and PILS water-soluble BrC absorption
239 that broadly remained stable for a smoke age up to 9 h (Sullivan et al., 2022).

240 Our results are broadly consistent with ~~the other published results~~ measurements from
241 ~~the~~ FIREX-AQ ~~campaign~~ and WE-CAN that sampled fresh plumes, and differ from the previous
242 studies that ~~examined longer plume ages sampled more aged smoke~~. The relatively
243 narrow limited plume age range of the FIREX-AQ sampling makes it challenging to deduce long-
244 term trends associated with changes in total absorption as a function of transport time. In addition,
245 the disparity in $\Delta\text{Abs}_{\lambda, \text{BrC}}/\Delta\text{CO}$ time dependence between FIREX-AQ observations and those
246 reported by Forrister et al. (2015) may be attributed to i) FIREX-AQ having sampled a greater
247 number of western U.S forest fires; and ii) the younger age of the FIREX-AQ plumes. More in-
248 flight sampling would be required to observe BrC absorption of plume ages 5 h to 50 h to determine

249 if the results observed by Forrister et al. (2015) would also show variability with a greater number
250 of fires, or if the BrC lifetime would converge to a similar value.

251 **3.2 3.2 Chemical evolution of brown carbon with plume age**

252 – Chromophores <500 Da were responsible for most of the absorption at 250-300 nm
253 measured in the aqueous samples (Figure 2, Figure ~~S7~~~~. When pooling all S11~~). For the 47 samples,
254 molecular species >500 Da contributed an average of 3.0 ± 1.9 % to total measured absorption at
255 250 nm, while molecular species <500 Da contributed an average of 72 ± 4.5 %. Absorption past
256 the exclusion volume represents an unidentified MW, as elution past this retention time (Figure
257 S3) indicates non-SEC analyte-column interactions were occurring. The average contribution to
258 total measured absorption by undefined MW species was 25.1 ± 5.7 %. Previous SEC-UV analyses
259 have observed elution beyond the exclusion volume and non-size exclusion effects- (Wong et al.,
260 2017; Lyu et al., 2021). Elution at later retention times has also been observed for fresh BrC
261 separated in a mobile phase ~~also~~ containing 50% acetonitrile (Lyu et al., 2021). This result was
262 attributed to non-size exclusion effects, such as hydrophobic interactions of BrC with the SEC
263 stationary phase, which may also have contributed to elution past the exclusion volume in our
264 samples. The absorption density plots of the aqueous samples from the flights listed in Table S1
265 had similar size-resolved features with varying magnitude in absorption (Figure ~~S7~~~~S5~~).

266 These results are the first reported SEC-UV measurements of very fresh (0-5 h) field
267 samples of biomass burning smoke, and they confirm some of the ~~trends~~observations from field
268 studies that measured more aged smoke, as well as laboratory studies that generated fresh or aged
269 smoke. Previous studies that examined biomass burning BrC using SEC-UV have similarly
270 concluded that fresh, less aged smoke contains a large fraction of lower MW absorbing species
271 (Di Lorenzo et al., 2017; Wong et al., 2017; Lyu et al., 2021). In the examination of field samples,
272 Di Lorenzo et al. (2017) collected ambient biomass burning aerosols that had been aged 10 to >72
273 h. They observed that low MW (<500 Da) chromophores contributed more to total absorption than
274 higher MW (>500 Da) compounds in the least aged (10 to 15 h) biomass burning-derived filter
275 extracts (Di Lorenzo et al., 2017). These findings resemble the absorption features of our FIREX-
276 AQ samples, which span a plume age range from 0 to 5 hours. Wong et al. (2019) collected used
277 SEC-UV to analyze filter extracts collected during fire seasons in Greece ~~that correspond to an~~
278 with atmospheric aging time rangeages of 1 to ~70 h, ~~analyzed with SEC-UV~~, and observed that
279 high MW species dominated total BrC absorption of the fresh and aged smoke. ~~The FIREX-AQ~~

280 ~~aqueous samples represent the first water-soluble BrC collected in solution downwind of western~~
281 ~~U.S. wildfires.~~ Differences between the FIREX-AQ aqueous samples and the results presented by
282 Wong et al. (2019) can be driven by varying types of fuel emissions, photochemical conditions,
283 meteorology, and differences in back trajectory analyses.

284 Two studies have applied SEC-UV analysis to lab-generated or lab-aged smoke samples.
285 Wong et al. (2017) pyrolyzed dry hardwood and aged the samples from 0 to 10 h with UV light.
286 They found that low MW chromophores dominated total absorption compared to high MW
287 species, which is generally consistent with our observations. Lyu et al. (2021) generated biomass
288 burning aerosol from laboratory combustion of boreal peat and also analyzed the aerosol by SEC-
289 UV. Under the same SEC-UV separation conditions, the FIREX-AQ water aqueous samples
290 parallel the findings of Lyu et al. (2021), with low MW BrC chromophores dominating total
291 absorption for unaged fresh smoke and smoke aged between 0 to 5 h in the atmosphere.

292 **3.3 Comparison of SEC-UV and BrC-PILS absorption**

293 Online and offline absorption sampling are complimentary. The online sampling by the
294 BrC-PILS provides continuous data with much higher time resolution (reported at 10 s), but it is
295 limited to two measurements: water-soluble absorption as a function of wavelength and water-
296 soluble organic carbon concentration. In contrast, ~~the~~ offline samples can be examined using SEC-
297 UV, C₁₈ chromatography, and other analytical techniques that are not feasible onboard an aircraft.
298 During FIREX-AQ, the BrC-PILS measured online water-soluble absorption in the same aqueous
299 flow that was collected for offline sampling. These are the only BrC samples whose absorption
300 was measured online and then subsequently offline during FIREX-AQ. ~~A comparison of the water-~~
301 ~~soluble absorption measured by the BrC-PILS, and the SEC-UV analysis are shown in Figure 3.~~
302 ~~Due to logistical constraints during FIREX AQ, a reference solution was not routinely run on the~~
303 ~~BrC-PILS instrument or the SEC-UV method to characterize the total absorption observed by both~~
304 ~~instruments.~~

305 We observe ~~two major~~ differences between the online and offline samples. First,
306 ~~the absorption by the offline SEC-UV at wavelengths greater than 300 nm did not exceed its~~
307 ~~detection limit. To facilitate comparison of absorption magnitudes, a power law fit was applied to~~
308 ~~the BrC-PILS absorption between 315–395 nm to extrapolate absorption to 300 nm (Figure 3).~~
309 The total absorption by the SEC-UV measurements is approximately an order of magnitude greater
310 than the BrC-PILS measurements at 300 nm. ~~Second, the BrC-PILS measured BrC absorption~~

311 between 310 and 500 nm. Although the SEC-UV measured between 190 and 800 nm, no
312 absorption distinguishable from the blanks was observed above 310 nm. The comparison between
313 the offline and online (Figure 3). To determine if the differences could be attributed to differences
314 in the diode array detector from the SEC-UV analysis and the BrC-PILS spectrometer, a standard
315 solution of 4-nitrocatechol was run on both systems in pure water (without the SEC column in line
316 and bypassing the PILS). At 350 nm, the agreement between the online, offline, and literature
317 measurements of 4-nitrocatechol absorption was $\pm 2.1\%$ (Figure S13) (Hinrichs et al., 2016).

318 The comparison between the online and offline work presented here can be compared to
319 previous non-co-located online-offline intercomparison studies. Di Lorenzo et al. (2017) compared
320 offline absorption measurements by SEC-UV of filter extracts by SEC-UV to PILS-LWCC online
321 measurements during the Southern Oxidant and Aerosol Study (SOAS). Although the SEC-UV
322 offline samples and online measurements during SOAS were not co-located, they showed
323 reasonable agreement with moderate correlation. Neither method was consistently higher than the
324 other and the median ratio (SEC-UV offline to PILS-LWCC online) was 0.9 (Figure S8). In that
325 study, discrepancies between the offline and online measurements were attributed to differences
326 in locations and inlet characteristics, as well as the solubilization methods (extraction via
327 sonication in water for offline SEC-UV and collision with impaction plate for online PILS-
328 LWCC)a median ratio (SEC-UV offline at 300 nm to PILS-LWCC online at 365 nm) of 0.9 and
329 r^2 of 0.53 (Figure S12). (Di Lorenzo et al., 2017). Zeng et al. (2021) also present an online-offline
330 absorption comparison of water-soluble BrC collected on board the NASA DC-8 aircraft during
331 FIREX-AQ. Online absorption measurements by a LWCC and aqueous filter extracts injected onto
332 a LWCC offline showed good agreement at 365 nm ($r^2 = 0.84$). The correlation suggested that the
333 filter measurement of BrC is not significantly influenced by possible sampling artifacts associated
334 with absorption of gases or evaporative loss of BrC components associated with filter collection
335 (Zeng et al., 2021).

336 Differences observed in the FIREX-AQ aqueous samples, and the previous comparison
337 between the online-offline BrC samples indicate the necessity to investigate a potential explanation
338 for these inconsistencies. Since the online BrC-PILS and offline SEC-UV samples represent the
339 same samples, solubilization differences between aerosol collection methods cannot explain the
340 variability observed between our measurements. We examine solvent effects as a potential
341 explanation. Although reasonable agreement between online measurements and offline filter

342 analyses has been demonstrated (Di Lorenzo et al., 2017; Zeng et al., 2021), Resch et al. (2023)
343 indicated that filter extracts that are not refrigerated immediately or extracts that remain
344 refrigerated for an extended storage time are susceptible to compositional changes. For logistical
345 reasons, our aqueous samples were collected into polypropylene tubes in the field and were not
346 immediately subjected to controlled refrigeration or to the SEC-UV analysis. The greater
347 absorption observed by the SEC-UV analysis (Figure 3) could reflect the possible hydrolysis of
348 oligomeric compounds stored in aqueous solution resulting in an increase the intensity of precursor
349 monomers as decomposition products (Resch et al., 2023). We consider this, as well as other
350 potential causes for the differences in the next section.

351 **3.4 Solvents affect Investigating the measured impact of solvent effects, pH, and storage** 352 **effects on absorption spectra**

353 The analysis of fresh biomass burning samples by SEC-UV may be affected by mobile
354 phase solvation effects, pH, and sample storage conditions. We analyze and discuss these variables
355 below and make recommendations for SEC-UV analysis. Plausible chemical structures of
356 chromophores responsible for BrC absorption have been identified and consist of conjugated
357 systems functionalized with hydroxyls, amines, nitro, carbonyls, and carboxylic acid groups
358 (Laskin et al., 2015; Hems et al., 2021; Lin et al., 2017; Fleming et al., 2020; Zeng et al., 2020b;
359 Hettiyadura et al., 2021; Marrero-Ortiz et al., 2019; De Haan et al., 2018; Ji et al., 2022). ~~To~~
360 compare the online and offline measurements, an assessment of The molecular complexities of BrC
361 species may be susceptible to changes in the absorption spectra depending on the analysis
362 conditions.

363 First, we assess solvation effects due to changes in the mobile phase ~~were considered. For~~
364 ~~the online measurements, the~~ composition. The PILS solubilizes BrC in pure water for the online
365 measurements to facilitate absorption measurements (Weber et al., 2001). ~~The~~ In contrast, the
366 mobile phase used for the offline SEC-UV analysis was a mixture of ~~a buffer solution and~~
367 ~~acetonitrile, and DIW with 25 mM ammonium acetate.~~ Chromatographic packing materials are
368 often ~~not compatible~~ incompatible with pure water and require a mixture with an organic solvent
369 to elute compounds from the stationary phase, or, in SEC separations, to prevent ~~disrupt~~
370 ~~partitioning or adsorption in an SEC column~~ adsorption to the stationary phase. For this reason,
371 chromatographic partitioning-based separations occur in aqueous-organic mixtures, where the
372 composition can be deliberately modified to optimize interactions of the target molecules between

373 the stationary phase and mobile phase. ~~Organic solvents can impact both molecular structure of~~
374 ~~BrC chromophores and their absorption properties. Since BrC is comprised of a variety of~~
375 ~~compounds, each component's ability to be solvated depends on the molecular structure of the~~
376 ~~BrC constituent and on the solvent (Chen et al., 2022). For instance, methanol is commonly used~~
377 ~~as a BrC extraction solvent due to its efficiency in extracting oxygenated compounds (Chen and~~
378 ~~Bond, 2010). Methanol is commonly used as a mobile phase component in liquid chromatographic~~
379 ~~separations. However, methanol can introduce artifacts and alter molecular structures. For~~
380 ~~example, methanol can react with carbonyl groups to form new structures such as esters, acetals,~~
381 ~~and hemiacetals (Walser et al., 2008; Bateman et al., 2008; Chen et al., 2022)~~In SEC, non-size
382 exclusion interactions between the analyte and stationary phase are dominated by electrostatic and
383 hydrophobic interactions (Hong et al., 2012). If the analyte and stationary phase are identically
384 charged, ion exclusion effects can occur, resulting in an earlier elution time as the analyte is
385 prevented from entering the pores. If the analyte and stationary phase are oppositely charged,
386 adsorption can result, leading to a later elution time. Hydrophobic effects can occur if the analyte
387 interacts with hydrophobic sites of the column matrix (Hong et al., 2012). The purpose of adding
388 ammonium acetate to the mobile phase is to increase the ionic strength of the mobile phase and
389 facilitate ion-pairing, which suppresses electrostatic interactions between the stationary phase and
390 the polar and charged functional groups. The organic solvent used in our mobile phase was
391 acetonitrile, which has been shown to be unreactive towards typical BrC components and has been
392 recommended as an inert solvent for BrC extraction and analysis (Walser et al., 2008; Bateman et
393 al., 2008; Chen et al., 2022). ~~The mobile phase solvent used here was acetonitrile, for which~~
394 ~~reactions with typical BrC components have not been observed and has been recommended as a~~
395 ~~more inert solvent for extraction and analysis (Walser et al., 2008; Bateman et al., 2008; Chen et~~
396 ~~al., 2022), yet offers a similar dielectric potential and intermolecular interactions between solvent~~
397 ~~and solute. Thus, this is unlikely to be the source of the absorption differences observed between~~
398 ~~the online and offline measurements in our work.~~ Therefore, we do not expect the mobile phase to
399 chemically alter BrC compounds while effective at mitigating column stationary phase-analyte
400 interactions.

401 ~~To assess whether solvent absorption effects could account for our online and offline~~
402 ~~differences, a standard solution of 4-nitrocatechol was run on both the BrC-PILS using water only~~
403 ~~and bypassing the PILS. The solution only passed through the LWCC and spectrophotometer as a~~

404 result. This 4-nitrocatechol solution was also injected into the diode array detector without the
405 SEC column in water and other mobile phases (Figure 4A). The absorption magnitude and
406 wavelength distribution for 4-nitrocatechol were comparable between the literature absorption
407 spectrum and the offline and online measurements when made in water (Hinrichs et al., 2016).
408 Absorption of 4-nitrocatechol changed when the water-acetonitrile mixture was used as the mobile
409 phase, with the absorption maximum red-shifting by approximately 100 nm. While chemical
410 changes caused by our mobile phase are unlikely, it is possible that other solvent effects on
411 absorption could be occurring. Effects of solvent on molecular absorption are well established in
412 the photochemistry literature (Lignell et al., 2014; Mo et al., 2017; Zheng et al., 2018; Lyu et al.,
413 2021; Chen et al., 2022; Dalton et al., 2023). The polarity of the solvent affects the absorption
414 wavelength by changing stabilization of the ground and/or excited states. ~~Our observation is~~
415 ~~consistent with decreased solvent polarity of acetonitrile-water (relative to water) leading to~~
416 ~~decreased stabilization of the ground state of the transition in 4-nitrocatechol. However, this effect~~
417 ~~is molecule dependent, as another BrC constituent, *o*-cresol, showed similar absorption spectra in~~
418 ~~both acetonitrile and water (Zheng et al., 2018). A biomass burning derived sample does not~~
419 ~~contain only a single compound, but is rather a complex combination of various compounds~~
420 ~~including aromatic organic acids, nitroaromatics, flavonoids, and polycyclic aromatic~~
421 ~~hydrocarbons (Lin et al., 2018; Fleming et al., 2020), each of which will have unique solvent~~
422 ~~absorption effects. We examined the effects of solvent on absorption of the complex environmental~~
423 ~~mixture Suwanee River Fulvic Acid (SRFA II; International Humic Substances Society, Saint~~
424 ~~Paul, MN, USA), which is a reference material that contains a mixture of molecules with~~
425 ~~absorption properties comparable to BrC (Figure 4B). As expected, we observed differences in~~
426 ~~absorption intensity and wavelength in the different solvents. Notably, we observed that absorption~~
427 ~~in acetonitrile-water was blue-shifted and changed in intensity relative to absorption in water. The~~
428 ~~intensity in acetonitrile-water was higher at shorter wavelengths and lower at longer wavelengths.~~
429 ~~If the BrC in our samples was subject to similar effects, this could explain some or all of the~~
430 ~~differences we observed between online and offline measurements, namely the reduced absorption~~
431 ~~at longer wavelengths and greater absorption at shorter wavelengths in the offline SEC-UV~~
432 ~~analysis. This demonstrates that careful consideration of potential solvent effects is required in any~~
433 ~~comparison of online and offline measurements, particularly between datasets.~~With a decrease in
434 solvent polarity, (acetonitrile-water is less polar relative to pure water), this can lead to a decrease

435 in stabilization of the ground state of BrC compounds (such as 4-nitrocatechol), but this effect is
436 molecule-dependent. The impact of solvation on red and blue spectral shifting will likely be several
437 nanometers, which could contribute to the observed differences in the offline and online absorption
438 measurements. Previous work has shown that acetonitrile could disrupt π - π interactions between
439 BrC molecules, which could cause the liberation of adsorbed low MW BrC chromophores from
440 larger chromophores or disrupt BrC aggregates (Lyu et al., 2021). Smaller, less conjugated systems
441 typically absorb in the ultraviolet-blue wavelength region, and their $\pi \rightarrow \pi^*$ transition red shifts
442 when more conjugated systems are fused together (Gorkowski et al., 2022). Thus, we would expect
443 absorption measurements in the presence of acetonitrile to be blue-shifted relative to those in pure
444 water. This represents a possible explanation for greater absorption intensity at lower wavelengths
445 measured in the offline SEC-UV analysis compared to the online analysis.

446 Second, we assess the pH of the sample matrix, which is known to affect the absorption profile
447 of BrC compounds. Multiple studies have investigated the impact of pH on wavelength-dependent
448 absorption. For example, Phillips et al. (2017) directly adjusted the pH of SRFA and biomass-
449 burning derived aqueous extracts (with sodium hydroxide or hydrochloric acid) and observed no
450 measurable shift in the spectra to shorter or longer wavelengths; however they did observe that as
451 the pH increased, there was an increase in the magnitude of absorption, which was more
452 pronounced at higher wavelengths. The pH of the default mobile phase solution was 7.2, while the
453 pH of the deionized water solutions in the PILS was approximately 5 (due to carbon dioxide
454 dissolution). To investigate the impact pH has on BrC absorption, we measured several compounds
455 that have been shown to contribute to BrC absorption (4-nitrocatechol, vanillin, 7-
456 hydroxycoumarin, 4-hydroxy-3-methoxy cinnamaldehyde, and mixture of the four compounds)
457 under different solvent and pH conditions: DIW, DIW with 25 mM ammonium acetate, as well as
458 the mobile phase at pH 5, 7.2, and 9. When the matrix conditions have a pH greater than the pK_a
459 of the compound in question, the species will deprotonate, resulting in a shift to longer wavelengths
460 (Hinrichs et al., 2016). For compounds with a pK_a between 5 and 9 (i.e., 4-nitrocatechol, 7-
461 hydroxycoumarin, vanillin), we observed this phenomenon (Figure S6). To assess the impact of
462 pH and mobile phase on a complex mixture, we also measured the absorption of a SRFA aqueous
463 solution and a FIREX-AQ aqueous sample with the abovementioned mobile phases (Figure 4 and
464 Figure S8). In contrast to the individual BrC compounds, no major changes in the spectral shape
465 were observed under different mobile phase conditions. To confirm these results, we measured the

466 absorption of SRFA in each solvent using a separate spectrophotometer (Figure S7). This suggests
467 that the pK_a of the majority of functional groups in the absorbing compounds present were less
468 than 5 or above 9. Nitroaromatic compounds typically have pK_a values between 5 and 8;
469 suggesting low levels of this class of compounds present in the aqueous samples. This observation
470 is comparable to the online BrC-PILS analysis; for aqueous absorption, Washenfelder et al. (2022)
471 observed the average absorption contribution at 365 nm of 4-nitrocatechol was less than 1.1 % and
472 the summed contribution to absorption by 2-nitrophenol, 4-nitrophenol, 4-nitrocatechol, 4-
473 nitroguaiacol, and 2,4-dinitrophenolate was less than 3.6 %. Since the absorption profile of SRFA
474 and the FIREX-AQ sample appear similar in all mobile phase conditions, we have no evidence
475 that pH of the mobile phase in the SEC separation conditions impacts the wavelength dependent
476 absorption of the FIREX-AQ aqueous samples.

477 Third, we assess the potential effect of storage on the aqueous samples measured by SEC-UV.
478 A recent study by Resch et al. (2023) observed that biomass burning-derived filter extracts stored
479 at temperatures above freezing may undergo compositional changes that can increase in signal for
480 various compounds. Hydrolysis reactions include converting alkenes to alcohols and esters to
481 carboxylic acids, and the breakdown of oligomers. The hydrolysis of oligomers such as dimer
482 esters stored in an aqueous solution can result in an increase in precursor monomers as
483 decomposition products leading to an increase in signal (Zhao et al., 2018; Resch et al., 2023).
484 Further, ammonium and alkylamines have been observed in high levels in biomass burning
485 aerosols (Di Lorenzo et al., 2018); aqueous reactions between dicarbonyls (e.g., glyoxal,
486 methylglyoxal) with ammonium and amines may also contribute to an increase in absorption
487 intensity at pH 4 to 7 (Powelson et al., 2014; Yang et al., 2023). The FIREX-AQ aqueous samples
488 had a pH of 5 and were stored at 4 °C for two years prior to analysis. Assuming they contained
489 dicarbonyl compounds and reduced nitrogenous species, it is possible reactions leading to products
490 that can contribute to greater absorption during storage occurred. To further investigate the impacts
491 of storage on a complex aqueous mixture, we measured the absorption spectra of two SRFA
492 solutions: one freshly made and one stored for one year at 4 °C. We observed an increase in
493 absorption in the aged SRFA solution, in which integrated absorption was 39 % higher than the
494 freshly-made solution. This same effect was also observed with SRHA solutions (Figure S14).
495 Thus, it is possible that processes during storage could have led to increased absorption measured
496 in the offline SEC samples.

497 Among the three processes discussed here, we conclude that the storage of aqueous extracts is
498 the most plausible explanation for the higher absorption observed in the offline samples from
499 FIREX-AQ. If hydrolysis reactions are occurring, we might expect this to impact the MW profile
500 (i.e., SEC elution times). We examined the MW profile of freshly-made and one year-aged SRFA
501 solutions (Figure 4C). The increase in absorption with storage does not measurably affect the
502 molecular size-resolved absorption of the mixtures. The same effect was observed for SRHA
503 (Figure S14). This demonstrates that any storage-induced changes in these complex mixtures of
504 organic molecules have a minimal impact on the molecular weight relative to the wide MW range
505 of the SEC column. The MW of the BrC species would have to change by ~ 100 Da to be noticeable
506 on the MW scale of our separation (250 Da to 75 kDa). Such a drastic change in MW is unlikely
507 the case in most hydrolysis reactions. Thus, our results above in which we broadly categorize MW
508 species to be less than or greater than 500 Da are likely robust. The SEC separation of the aqueous
509 samples signify that low MW (<500 Da) chromophores contribute more to total absorption than
510 higher MW (>500 Da), this finding is supported by previous SEC-UV analyses of BrC aged less
511 than 10 hrs (Di Lorenzo et al., 2017; Lyu et al., 2021). The consistent MW profiles between the
512 freshly-made and stored solutions of SRFA and SRHA reasonably suggest that storage did not
513 have a major impact on the MW of BrC.

514 **4. Conclusions and implications**

515 During FIREX-AQ, instruments onboard the NOAA Twin Otter aircraft sampled smoke
516 plumes from wildfires in the western United States with plume ages of 0 to 5 h. The BrC-PILS
517 measured water-soluble BrC absorption online and collected aerosol in aqueous solution for offline
518 SEC-UV analysis. The aqueous samples were collected during downwind plume transects and the
519 online data was collected continuously during inflight sampling. SEC-UV analysis shows that BrC
520 absorption was dominated by chromophores <500 Da. This finding is consistent with reports of
521 laboratory-generated fresh smoke samples. Integrated absorption at 300 nm from the SEC-UV
522 analysis was used to calculate trends in normalized BrC absorption as a function of plume age.
523 These trends were variable and did not show an exponential decay, which is consistent with
524 recently published results from the FIREX-AQ field campaign that examined normalized BrC
525 absorption trends for plumes over 0 to 10 h. Comparison of the online and offline analyses of the
526 same aqueous extracts reveals discrepancies, specifically higher absorption intensity and

527 absorption at lower wavelengths. These discrepancies between online and offline samples
528 demonstrate the importance of solvent effects, considering the conditions in which were
529 demonstrated through the absorption measurements under different solvent conditions. This
530 highlights the importance of careful consideration of potential solvent effects when comparing
531 online and are made. The inconsistencies between the offline SEC-UV analysis and the online
532 measurements of BrC and when assessing BrC solubility. Offline are not explained by pH or
533 solvent effects, but may be due to reactions occurring during storage. Although increases in
534 absorption measurement conditions can alter the molecular structural of BrC constituents and may
535 occur during storage of aqueous solutions, it is less likely to impact the wavelength dependence of
536 the MW of the FIREX-AQ BrC species. This highlights that BrC species are more stable collected
537 on filters rather than in aqueous solution and the importance of inter-comparison absorption
538 measurements by multiple methods.

539

540 **Acknowledgements**

541 We thank Carsten Warneke, Joshua Schwarz, James Crawford, and Jack Dibb for organizing the
542 FIREX-AQ field campaign. We thank the NOAA Aircraft Operations Center for support during
543 the field mission. L.A. was supported by a Mitacs Globalink Research Internship and an NSERC
544 Discovery Grant. The FIREX-AQ project was supported by the NOAA Atmospheric Chemistry,
545 Carbon, and Climate Program (AC4). We thank Robert Di Lorenzo and Trevor VandenBoer for
546 helpful discussions. We thank three anonymous reviewers for their insightful feedback.

547 **Data Availability Statement**

548 The data used in the study are publicly available at [https://www-air.larc.nasa.gov/missions/firex-](https://www-air.larc.nasa.gov/missions/firex-aq/)
549 [aq/](https://www-air.larc.nasa.gov/missions/firex-aq/)

550 **Competing Interests**

551 At least one of the (co-)authors is a member of the editorial board of Atmospheric Chemistry and
552 Physics.

553 **References**

554 Andreae, M. O. and Gelencsér, A.: Black carbon or brown carbon? The nature of light-absorbing
555 carbonaceous aerosols, *Atmospheric Chemistry & Physics*, 6, 3131–3148,
556 <https://doi.org/10.5194/acp-6-3131-2006>, 2006.

557 Bateman, A. P., Walser, M. L., Desyaterik, Y., Laskin, J., Laskin, A., and Nizkorodov, S. A.:
558 The effect of solvent on the analysis of secondary organic aerosol using electrospray ionization
559 mass spectrometry., *Environ Sci Technol*, 42, 7341–7346, <https://doi.org/10.1021/es801226w>,
560 2008.

561 Bluvshstein, N., Lin, P., Flores, M., Segev, L., Mazar, Y., Tas, E., Snider, G., Weagle, C., Brown,
562 S., Laskin, A., and Rudich, Y.: Broadband optical properties of biomass burning aerosol and
563 identification of brown carbon chromophores, *Journal of Geophysical Research: Atmospheres*,
564 122, 5441–5456, <https://doi.org/10.1002/2016JD026230>, 2017.

565 Bond, T. C., Streets, D. G., Yarber, K. F., Nelson, S. M., Woo, J.-H., and Klimont, Z.: A
566 technology-based global inventory of black and organic carbon emissions from combustion,
567 *Journal of Geophysical Research: Atmospheres*, 109, <https://doi.org/10.1029/2003JD003697>,
568 2004.

569 Boucher, O.; Randall, D.; Artaxo, P.; Bretherton, C.; Feingold, G. ; Forster, P.; Kerminen, V.
570 M.; Kondo, Y.; Liao, H.; Lohmann, U. ; and Rasch, P.; Satheesh, S. K.; Sherwood, S.; Stevens,
571 B.; Zhang, X. Y.: Clouds and Aerosols. In: *Climate Change 2013: The Physical Science Basis*.
572 Contribution of Working Group I to the Fifth Assessment Report of the Intergovernmental Panel
573 on Climate Change, in: *Climate Change 2013: The Physical Science Basis. Contribution of*
574 *Working Group I to the Fifth Assessment Report of the Intergovernmental Panel on Climate*
575 *Change*, Cambridge University Press:, New York, NY, 2013.

576 [Buis, A.: The Climate Connections of a Record Fire Year in the U.S. West—Climate Change:
577 Vital Signs of the Planet: \[https://climate.nasa.gov/blog/3066/the-climate-connections-of-a-
578 record-fire-year-in-the-us-west/\]\(https://climate.nasa.gov/blog/3066/the-climate-connections-of-a-
578 record-fire-year-in-the-us-west/\), 2021.](https://climate.nasa.gov/blog/3066/the-climate-connections-of-a-record-fire-year-in-the-us-west/)

579 Chen, K., Raeofy, N., Lum, M., Mayorga, R., Woods, M., Bahreini, R., Zhang, H., and Lin, Y.-
580 H.: Solvent effects on chemical composition and optical properties of extracted secondary brown

581 carbon constituents, *Aerosol Science and Technology*, 56, 917–930,
582 <https://doi.org/10.1080/02786826.2022.2100734>, 2022.

583 ~~[Chen, Y. and Bond, T. C.: Light absorption by organic carbon from wood combustion,](#)~~
584 ~~[Atmospheric Chemistry and Physics](#), 10, 1773–1787, <https://doi.org/10.5194/acp-10-1773-2010>,~~
585 ~~[2010.](#)~~

586 Crosson, E. R.: A cavity ring-down analyzer for measuring atmospheric levels of methane,
587 carbon dioxide, and water vapor, *Applied Physics B*, 92, 403–408,
588 <https://doi.org/10.1007/s00340-008-3135-y>, 2008.

589 Dalton, A. B., Le, S. M., Karimova, N. V., Gerber, R. B., and Nizkorodov, S. A.: Influence of
590 solvent on the electronic structure and the photochemistry of nitrophenols, *Environ. Sci.: Atmos.*,
591 3, 257–267, <https://doi.org/10.1039/D2EA00144F>, 2023.

592 De Haan, D. O., Tapavicza, E., Riva, M., Cui, T., Surratt, J. D., Smith, A. C., Jordan, M.-C.,
593 Nilakantan, S., Almodovar, M., Stewart, T. N., de Loera, A., De Haan, A. C., Cazaunau, M.,
594 Gratien, A., Pangui, E., and Doussin, J.-F.: Nitrogen-containing, light-absorbing oligomers
595 produced in aerosol particles exposed to methylglyoxal, photolysis, and cloud cycling, *Environ.*
596 *Sci. Technol.*, 52, 4061–4071, <https://doi.org/10.1021/acs.est.7b06105>, 2018.

597 Di Lorenzo, R. A. and Young, C. J.: Size separation method for absorption characterization in
598 brown carbon: Application to an aged biomass burning sample, *Geophysical Research Letters*,
599 43, 458–465, <https://doi.org/10.1002/2015GL066954>, 2016.

600 Di Lorenzo, R. A., Washenfelder, R. A., Attwood, A. R., Guo, H., Xu, L., Ng, N. L., Weber, R.
601 J., Baumann, K., Edgerton, E., and Young, C. J.: Molecular-size-separated brown carbon
602 absorption for biomass-burning aerosol at multiple field sites, *Environmental Science and*
603 *Technology*, 51, 3128–3137, <https://doi.org/10.1021/acs.est.6b06160>, 2017.

604 ~~[Di Lorenzo, R. A., Place, B. K., VandenBoer, T. C., and Young, C. J.: Composition of Size-](#)~~
605 ~~[Resolved Aged Boreal Fire Aerosols: Brown Carbon, Biomass Burning Tracers, and Reduced](#)~~
606 ~~[Nitrogen, *ACS Earth and Space Chemistry*, 2, 278–285,](#)~~
607 ~~<https://doi.org/10.1021/acsearthspacechem.7b00137>, 2018.~~

608 Feng, Y., Ramanathan, V., and Kotamarthi, V. R.: Brown carbon: a significant atmospheric
609 absorber of solar radiation?, *Atmospheric Chemistry and Physics*, 13, 8607–8621,
610 <https://doi.org/10.5194/acp-13-8607-2013>, 2013.

611 Finewax, Z., de Gouw, J. A., and Ziemann, P. J.: Identification and quantification of 4-
612 nitrocatechol formed from OH and NO₃ radical-initiated reactions of catechol in air in the
613 presence of NO_x: implications for secondary organic aerosol formation from biomass burning,
614 *Environ. Sci. Technol.*, 52, 1981–1989, <https://doi.org/10.1021/acs.est.7b05864>, 2018.

615 Fleming, L. T., Lin, P., Roberts, J. M., Selimovic, V., Yokelson, R., Laskin, J., Laskin, A., and
616 Nizkorodov, S. A.: Molecular composition and photochemical lifetimes of brown carbon
617 chromophores in biomass burning organic aerosol, *Atmospheric Chemistry and Physics*, 20,
618 1105–1129, <https://doi.org/10.5194/acp-20-1105-2020>, 2020.

619 Forrister, H., Liu, J., Scheuer, E., Dibb, J., Ziemba, L., Thornhill, K. L., Anderson, B., Diskin,
620 G., Perring, A. E., Schwarz, J. P., Campuzano-Jost, P., Day, D. A., Palm, B. B., Jimenez, J. L.,
621 Nenes, A., and Weber, R. J.: Evolution of brown carbon in wildfire plumes, *Geophysical*
622 *Research Letters*, 42, 4623–4630, <https://doi.org/10.1002/2015GL063897>, 2015.

623 Forster, P.; Ramaswamy, V.; Artaxo, P.; Berntsen, T.; Betts, R. ;, Fahey, D. W.; Haywood, J.;
624 Lean, J.; Lowe, D. C.; Myhre, G. ; N., and J.; Prinn, R.; Raga, G.; Schulz, M.; Van Dorland, R.:
625 In *Climate Change 2007: The Physical Science Basis. Contribution of Working Group I to the*
626 *Fourth Assessment Report of the Intergovernmental Panel on Climate Change*, Cambridge
627 University Press: Cambridge, United Kingdom and New York, NY, 2007; pp 129–243, 2007.

628 [Gorkowski, K., Benedict, K. B., Carrico, C. M., and Dubey, M. K.: Complexities in Modeling](https://doi.org/10.1021/acs.jpca.2c02236)
629 [Organic Aerosol Light Absorption., *J Phys Chem A*, 126, 4827–4833,](https://doi.org/10.1021/acs.jpca.2c02236)
630 <https://doi.org/10.1021/acs.jpca.2c02236>, 2022.

631 Harrison, M. A. J., Barra, S., Borghesi, D., Vione, D., Arsene, C., and Iulian Olariu, R.: Nitrated
632 phenols in the atmosphere: a review, *Atmospheric Environment*, 39, 231–248,
633 <https://doi.org/10.1016/j.atmosenv.2004.09.044>, 2005.

634 Hems, R. F., Schnitzler, E. G., Liu-Kang, C., Cappa, C. D., and Abbatt, J. P. D.: Aging of
635 atmospheric brown carbon aerosol, *ACS Earth and Space Chemistry*, 5, 722–748,
636 <https://doi.org/10.1021/acsearthspacechem.0c00346>, 2021.

637 Hettiyadura, A. P. S., Garcia, V., Li, C., West, C. P., Tomlin, J., He, Q., Rudich, Y., and Laskin,
638 A.: Chemical composition and molecular-specific optical properties of atmospheric brown
639 carbon associated with biomass burning., *Environ Sci Technol*, 55, 2511–2521,
640 <https://doi.org/10.1021/acs.est.0c05883>, 2021.

641 Hinrichs, R. Z., Buczek, P., and Trivedi, J. J.: Solar absorption by aerosol-bound nitrophenols
642 compared to aqueous and gaseous nitrophenols., *Environ Sci Technol*, 50, 5661–5667,
643 <https://doi.org/10.1021/acs.est.6b00302>, 2016.

644 [Hong, P., Koza, S., and Bouvier, E. S. P.: a review size-exclusion chromatography for the](#)
645 [analysis of protein biotherapeutics and their aggregates, *Journal of Liquid Chromatography &*](#)
646 [Related Technologies, 35, 2923–2950, <https://doi.org/10.1080/10826076.2012.743724>, 2012.](#)

647 Ji, Y., Shi, Q., Ma, X., Gao, L., Wang, J., Li, Y., Gao, Y., Li, G., Zhang, R., and An, T.:
648 Elucidating the critical oligomeric steps in secondary organic aerosol and brown carbon
649 formation, *Atmospheric Chemistry and Physics*, 22, 7259–7271, [https://doi.org/10.5194/acp-22-](https://doi.org/10.5194/acp-22-7259-2022)
650 [7259-2022](https://doi.org/10.5194/acp-22-7259-2022), 2022.

651 Karion, A., Sweeney, C., Wolter, S., Newberger, T., Chen, H., Andrews, A., Kofler, J., Neff, D.,
652 and Tans, P.: Long-term greenhouse gas measurements from aircraft, *Atmospheric Measurement*
653 *Techniques*, 6, 511–526, <https://doi.org/10.5194/amt-6-511-2013>, 2013.

654 Laskin, A., Laskin, J., and Nizkorodov, S. A.: Chemistry of Atmospheric Brown Carbon,
655 *Chemical Reviews*, 115, 4335–4382, <https://doi.org/10.1021/cr5006167>, 2015.

656 Liao, J., Wolfe, G. M., Hannun, R. A., St. Clair, J. M., Hanisco, T. F., Gilman, J. B., Lamplugh,
657 A., Selimovic, V., Diskin, G. S., Nowak, J. B., Halliday, H. S., DiGangi, J. P., Hall, S. R.,
658 Ullmann, K., Holmes, C. D., Fite, C. H., Agastra, A., Ryerson, T. B., Peischl, J., Bourgeois, I.,
659 Warneke, C., Coggon, M. M., Gkatzelis, G. I., Sekimoto, K., Fried, A., Richter, D., Weibring, P.,
660 Apel, E. C., Hornbrook, R. S., Brown, S. S., Womack, C. C., Robinson, M. A., Washenfelder, R.
661 A., Veres, P. R., and Neuman, J. A.: Formaldehyde evolution in US wildfire plumes during the
662 Fire Influence on Regional to Global Environments and Air Quality experiment (FIREX-AQ),
663 *Atmospheric Chemistry and Physics*, 21, 18319–18331, [https://doi.org/10.5194/acp-21-18319-](https://doi.org/10.5194/acp-21-18319-2021)
664 [2021](https://doi.org/10.5194/acp-21-18319-2021), 2021.

665 Lignell, H., Hinks, M. L., and Nizkorodov, S. A.: Exploring matrix effects on photochemistry of
666 organic aerosols, *Proceedings of the National Academy of Sciences*, 111, 13780–13785,
667 <https://doi.org/10.1073/pnas.1322106111>, 2014.

668 Lin, P., Bluvshstein, N., Rudich, Y., Nizkorodov, S. A., Laskin, J., and Laskin, A.: Molecular
669 chemistry of atmospheric brown carbon inferred from a nationwide biomass burning event,
670 *Environmental Science & Technology*, 51, 11561–11570,
671 <https://doi.org/10.1021/acs.est.7b02276>, 2017.

672 ~~Lin, P., Fleming, L. T., Nizkorodov, S. A., Laskin, J., and Laskin, A.: Comprehensive molecular~~
673 ~~characterization of atmospheric brown carbon by high-resolution mass spectrometry with~~
674 ~~electrospray and atmospheric pressure photoionization., *Anal Chem*, 90, 12493–12502,~~
675 ~~<https://doi.org/10.1021/acs.analchem.8b02177>, 2018.~~

676 Liu, J., Lin, P., Laskin, A., Laskin, J., Kathmann, S. M., Wise, M., Caylor, R., Imholt, F.,
677 Selimovic, V., and Shilling, J. E.: Optical properties and aging of light-absorbing secondary
678 organic aerosol, *Atmospheric Chemistry and Physics*, 16, 12815–12827,
679 <https://doi.org/10.5194/acp-16-12815-2016>, 2016.

680 Lyu, M., Thompson, D. K., Zhang, N., Cuss, C. W., Young, C. J., and Styler, S. A.: Unraveling
681 the complexity of atmospheric brown carbon produced by smoldering boreal peat using size-
682 exclusion chromatography with selective mobile phases, *Environ. Sci.: Atmos.*, 1, 241–252,
683 <https://doi.org/10.1039/D1EA00011J>, 2021.

684 Marlon, J. R., Bartlein, P. J., Gavin, D. G., Long, C. J., Anderson, R. S., Briles, C. E., Brown, K.
685 J., Colombaroli, D., Hallett, D. J., Power, M. J., Scharf, E. A., and Walsh, M. K.: Long-term
686 perspective on wildfires in the western USA, *Proceedings of the National Academy of Sciences*,
687 109, E535 LP-E543, <https://doi.org/10.1073/pnas.1112839109>, 2012.

688 Marrero-Ortiz, W., Hu, M., Du, Z., Ji, Y., Wang, Y., Guo, S., Lin, Y., Gomez-Hernandez, M.,
689 Peng, J., Li, Y., Secret, J., Zamora, M. L., Wang, Y., An, T., and Zhang, R.: Formation and
690 optical properties of brown carbon from small α -dicarbonyls and amines, *Environ. Sci. Technol.*,
691 53, 117–126, <https://doi.org/10.1021/acs.est.8b03995>, 2019.

692 Mo, Y., Li, J., Liu, J., Zhong, G., Cheng, Z., Tian, C., Chen, Y., and Zhang, G.: The influence of
693 solvent and pH on determination of the light absorption properties of water-soluble brown

694 carbon, *Atmospheric Environment*, 161, 90–98, <https://doi.org/10.1016/j.atmosenv.2017.04.037>,
695 2017.

696 Parks, S. A. and Abatzoglou, J. T.: Warmer and Drier Fire Seasons Contribute to Increases in
697 Area Burned at High Severity in Western US Forests From 1985 to 2017, *Geophysical Research*
698 *Letters*, 47, e2020GL089858, <https://doi.org/10.1029/2020GL089858>, 2020.

699 [Phillips, S. M., Bellcross, A. D., and Smith, G. D.: Light Absorption by Brown Carbon in the](#)
700 [Southeastern United States is pH-dependent, *Environ. Sci. Technol.*, 51, 6782–6790,](#)
701 <https://doi.org/10.1021/acs.est.7b01116>, 2017.

702 [Powelson, M. H., Espelien, B. M., Hawkins, L. N., Galloway, M. M., and De Haan, D. O.:](#)
703 [Brown Carbon Formation by Aqueous-Phase Carbonyl Compound Reactions with Amines and](#)
704 [Ammonium Sulfate, *Environ. Sci. Technol.*, 48, 985–993, <https://doi.org/10.1021/es4038325>,](#)
705 [2014.](#)

706 Ramanathan, V. and Carmichael, G.: Global and regional climate changes due to black carbon,
707 *Nat Geosci*, 1, <https://doi.org/10.1038/ngeo156>, 2008.

708 [Resch, J., Wolfer, K., Barth, A., and Kalberer, M.: Effects of storage conditions on the](#)
709 [molecular-level composition of organic aerosol particles, *Atmospheric Chemistry and Physics*,](#)
710 [23, 9161–9171, <https://doi.org/10.5194/acp-23-9161-2023>, 2023.](#)

711 Seinfeld, J. H. and Pankow, J. F.: Organic Atmospheric Particulate Material, *Annual Review of*
712 *Physical Chemistry*, 54, 121–140, <https://doi.org/10.1146/annurev.physchem.54.011002.103756>,
713 2003.

714 Simoneit, B. R. T.: Biomass burning — a review of organic tracers for smoke from incomplete
715 combustion, *Applied Geochemistry*, 17, 129–162, <https://doi.org/10.1016/S0883->
716 [2927\(01\)00061-0](#), 2002.

717 Smith, J. D., Sio, V., Yu, L., Zhang, Q., and Anastasio, C.: Secondary organic aerosol production
718 from aqueous reactions of atmospheric phenols with an organic triplet excited state,
719 *Environmental Science & Technology*, 48, 1049–1057, <https://doi.org/10.1021/es4045715>, 2014.

720 [Sullivan, A. P., Pokhrel, R. P., Shen, Y., Murphy, S. M., Toohey, D. W., Campos, T., Lindaas, J.,](#)
721 [Fischer, E. V., and Collett Jr., J. L.: Examination of brown carbon absorption from wildfires in](#)

722 [the western US during the WE-CAN study, *Atmospheric Chemistry and Physics*, 22, 13389–](#)
723 [13406, <https://doi.org/10.5194/acp-22-13389-2022>, 2022.](#)

724 Turpin, B. J., Cary, R. A., and Huntzicker, J. J.: An in situ, time-resolved analyzer for aerosol
725 organic and elemental carbon, *Aerosol Science and Technology*, 12, 161–171,
726 <https://doi.org/10.1080/02786829008959336>, 1990.

727 Walser, M. L., Desyaterik, Y., Laskin, J., Laskin, A., and Nizkorodov, S. A.: High-resolution
728 mass spectrometric analysis of secondary organic aerosol produced by ozonation of limonene,
729 *Phys. Chem. Chem. Phys.*, 10, 1009–1022, <https://doi.org/10.1039/B712620D>, 2008.

730 Warneke, C., Schwarz, J. P., Dibb, J., Kalashnikova, O., Frost, G., Al-Saad, J., Brown, S. S.,
731 Brewer, Wm. A., Soja, A., Seidel, F. C., Washenfelder, R. A., Wiggins, E. B., Moore, R. H.,
732 Anderson, B. E., Jordan, C., Yacovitch, T. I., Herndon, S. C., Liu, S., Kuwayama, T., Jaffe, D.,
733 Johnston, N., Selimovic, V., Yokelson, R., Giles, D. M., Holben, B. N., Goloub, P., Popovici, I.,
734 Trainer, M., Kumar, A., Pierce, R. B., Fahey, D., Roberts, J., Gargulinski, E. M., Peterson, D. A.,
735 Ye, X., Thapa, L. H., Saide, P. E., Fite, C. H., Holmes, C. D., Wang, S., Coggon, M. M., Decker,
736 Z. C. J., Stockwell, C. E., Xu, L., Gkatzelis, G., Aikin, K., Lefer, B., Kaspari, J., Griffin, D.,
737 Zeng, L., Weber, R., Hastings, M., Chai, J., Wolfe, G. M., Hanisco, T. F., Liao, J., Campuzano
738 Jost, P., Guo, H., Jimenez, J. L., Crawford, J., and The FIREX-AQ Science Team: Fire Influence
739 on Regional to Global Environments and Air Quality (FIREX-AQ), *Journal of Geophysical*
740 *Research: Atmospheres*, 128, e2022JD037758, <https://doi.org/10.1029/2022JD037758>, 2023.

741 Washenfelder, R., Attwood, A., Brock, C., Guo, H., Xu, L., Weber, R., Ng, N., Allen, H., Ayres,
742 B., Baumann, K., Cohen, R., Draper, D., Duffey, K., Edgerton, E., Fry, J., Hu, W., Jimenez, J.,
743 Palm, B., Romer, P., and Brown, S.: Biomass burning dominates brown carbon absorption in the
744 rural southeastern United States, *Geophysical Research Letters*, 42, 653–664,
745 <https://doi.org/10.1002/2014GL062444>, 2015.

746 Washenfelder, R. A., Azzarello, L., Ball, K., Brown, S. S., Decker, Z. C. J., Franchin, A.,
747 Fredrickson, C. D., Hayden, K., Holmes, C. D., Middlebrook, A. M., Palm, B. B., Pierce, R. B.,
748 Price, D. J., Roberts, J. M., Robinson, M. A., Thornton, J. A., Womack, C. C., and Young, C. J.:
749 Complexity in the evolution, composition, and spectroscopy of brown carbon in aircraft
750 measurements of wildfire plumes, *Geophysical Research Letters*, 49, e2022GL098951,
751 <https://doi.org/10.1029/2022GL098951>, 2022.

752 Weber, R. J., Orsini, D., Daun, Y., Lee, Y.-N., Klotz, P. J., and Brechtel, F.: A particle-into-
753 liquid collector for rapid measurement of aerosol bulk chemical composition, *Aerosol Science*
754 *and Technology*, 35, 718–727, <https://doi.org/10.1080/02786820152546761>, 2001.

755 van der Werf, G. R., Randerson, J. T., Giglio, L., Collatz, G. J., Mu, M., Kasibhatla, P. S.,
756 Morton, D. C., DeFries, R. S., Jin, Y., and van Leeuwen, T. T.: Global fire emissions and the
757 contribution of deforestation, savanna, forest, agricultural, and peat fires (1997–2009),
758 *Atmospheric Chemistry and Physics*, 10, 11707–11735, [https://doi.org/10.5194/acp-10-11707-](https://doi.org/10.5194/acp-10-11707-2010)
759 2010, 2010.

760 Wong, J. P. S., Nenes, A., and Weber, R. J.: Changes in light absorptivity of molecular weight
761 separated brown carbon due to photolytic aging, *Environmental Science & Technology*, 51,
762 8414–8421, <https://doi.org/10.1021/acs.est.7b01739>, 2017.

763 Wong, J. P. S., Tsagkaraki, M., Tsiodra, I., Mihalopoulos, N., Violaki, K., Kanakidou, M.,
764 Sciare, J., Nenes, A., and Weber, R. J.: Atmospheric evolution of molecular-weight-separated
765 brown carbon from biomass burning, *Atmospheric Chemistry and Physics*, 19, 7319–7334,
766 <https://doi.org/10.5194/acp-19-7319-2019>, 2019.

767 Xie, M., Chen, X., Hays, M. D., Lewandowski, M., Offenberg, J., Kleindienst, T. E., and Holder,
768 A. L.: Light Absorption of secondary organic aerosol: composition and contribution of
769 nitroaromatic compounds., *Environ Sci Technol*, 51, 11607–11616,
770 <https://doi.org/10.1021/acs.est.7b03263>, 2017.

771 Xie, M., Chen, X., Hays, M. D., and Holder, A. L.: Composition and light absorption of N-
772 containing aromatic compounds in organic aerosols from laboratory biomass burning,
773 *Atmospheric chemistry and physics*, 19, 2899–2915, <https://doi.org/10.5194/acp-19-2899-2019>,
774 2019.

775 [Yang, L., Huang, R.-J., Shen, J., Wang, T., Gong, Y., Yuan, W., Liu, Y., Huang, H., You, Q.,](#)
776 [Huang, D. D., and Huang, C.: New Insights into the Brown Carbon Chromophores and](#)
777 [Formation Pathways for Aqueous Reactions of \$\alpha\$ -Dicarbonyls with Amines and Ammonium,](#)
778 [Environ. Sci. Technol., 57, 12351–12361, https://doi.org/10.1021/acs.est.3c04133, 2023.](#)

779 Zeng, L., Zhang, A., Wang, Y., Wagner, N. L., Katich, J. M., Schwarz, J. P., Schill, G. P., Brock,
780 C., Froyd, K. D., Murphy, D. M., Williamson, C. J., Kupc, A., Scheuer, E., Dibb, J., and Weber,

781 R. J.: Global Measurements of Brown Carbon and Estimated Direct Radiative Effects., *Geophys*
782 *Res Lett*, 47, e2020GL088747, <https://doi.org/10.1029/2020GL088747>, 2020a.

783 Zeng, L., Sullivan, A. P., Washenfelder, R. A., Dibb, J., Scheuer, E., Campos, T. L., Katich, J.
784 M., Levin, E., Robinson, M. A., and Weber, R. J.: Assessment of online water-soluble brown
785 carbon measuring systems for aircraft sampling, *Atmospheric Measurement Techniques*, 14,
786 6357–6378, <https://doi.org/10.5194/amt-14-6357-2021>, 2021.

787 Zeng, L., Dibb, J., Scheuer, E., Katich, J. M., Schwarz, J. P., Bourgeois, I., Peischl, J., Ryerson,
788 T., Warneke, C., Perring, A. E., Diskin, G. S., DiGangi, J. P., Nowak, J. B., Moore, R. H.,
789 Wiggins, E. B., Pagonis, D., Guo, H., Campuzano-Jost, P., Jimenez, J. L., Xu, L., and Weber, R.
790 J.: Characteristics and evolution of brown carbon in western United States wildfires,
791 *Atmospheric Chemistry and Physics*, 22, 8009–8036, <https://doi.org/10.5194/acp-22-8009-2022>,
792 2022.

793 Zeng, Y., Shen, Z., Takahama, S., Zhang, L., Zhang, T., Lei, Y., Zhang, Q., Xu, H., Ning, Y.,
794 Huang, Y., Cao, J., and Rudolf, H.: Molecular absorption and evolution mechanisms of PM_{2.5}
795 brown carbon revealed by electrospray ionization fourier transform–ion cyclotron resonance
796 mass spectrometry during a severe winter pollution episode in Xi’an, China, *Geophysical*
797 *Research Letters*, 47, e2020GL087977, <https://doi.org/10.1029/2020GL087977>, 2020b.

798 Zhang, Y., Forrister, H., Liu, J., Dibb, J., Anderson, B., Schwarz, J. P., Perring, A. E., Jimenez, J.
799 L., Campuzano-Jost, P., Wang, Y., Nenes, A., and Weber, R. J.: Top-of-atmosphere radiative
800 forcing affected by brown carbon in the upper troposphere, *Nature Geoscience*, 10, 486–489,
801 <https://doi.org/10.1038/ngeo2960>, 2017.

802 [Zhao, R., Kenseth, C. M., Huang, Y., Dalleska, N. F., Kuang, X. M., Chen, J., Paulson, S. E.,](#)
803 [and Seinfeld, J. H.: Rapid Aqueous-Phase Hydrolysis of Ester Hydroperoxides Arising from](#)
804 [Criegee Intermediates and Organic Acids., *J Phys Chem A*, 122, 5190–5201,](#)
805 <https://doi.org/10.1021/acs.jpca.8b02195>, 2018.

806 Zheng, D., Yuan, X.-A., Ma, H., Li, X., Wang, X., Liu, Z., and Ma, J.: Unexpected solvent
807 effects on the UV/Vis absorption spectra of o-cresol in toluene and benzene: in contrast with
808 non-aromatic solvents, *Royal Society Open Science*, 5, 171928,
809 <https://doi.org/10.1098/rsos.171928>, 2018.

Absorption

810 **Figure 1.** Figure 1. Ratio of absorption measured by SEC-UV at 300 nm to CO enhancement
811 as a function of plume age for aqueous samples collected for six flights during FIREX-AQ 2019.
812 Absorption measured by SEC-UV with a mobile phase that consisted of equal parts acetonitrile
813 and 18.2 M Ω -cm deionized water with 25 mM ammonium acetate at a flow rate of 1 mL min⁻¹.

814 **Figure 2.** Figure 2. Absorption contribution at 300 nm of high (>500 Da), low (<500 Da),
815 and unidentified molecular weight species for aqueous samples collected during the second
816 flight leg on 21 Aug 2019.

817 **Figure 3.** Total absorption measured offline by the SEC-UV (at 300 nm) analysis compared to the
818 total absorption measured online by the BrC-PILS (averaged 310-320 nm)-extrapolated to 300 nm
819 using a power-law fit). Each colour represents a different flight leg and each marker represents the
820 total integrated absorption measured at 300 nm for each aqueous sample subjected to the
821 measured by SEC-UV analysis. The online BrC-PILS absorption measurement was averaged over
822 the collection time of each aqueous sample was. The error bars represent the total uncertainty in
823 the online and offline measurements.

824 **Figure 3.** Figure 4. Absorption as a function of wavelength of (a) SRFA and (b) a FIREX-
825 AQ aqueous sample collected on 28 Aug 2019 L3 with varying mobile phases. (c) Molecular
826 weight profile of a freshly-made 15 μ g/mL SRFA solution and the same solution one year later.
827 The shaded region represents the coefficient of variation for absorption at each wavelength using
828 n = 3 DIW.

829 **Figure 4.** (a) Absorption cross section of 4-nitrocatechol measured in solution measured using the
830 BrC-PILS (bypassing the PILS), the SEC-UV set-up bypassing the SEC column with two different
831 mobile phases, and by Hinrichs et al. (b) Absorption of fulvic acid measured with the SEC-UV
832 set-up bypassing the column in three different mobile phases.

Figure 1.

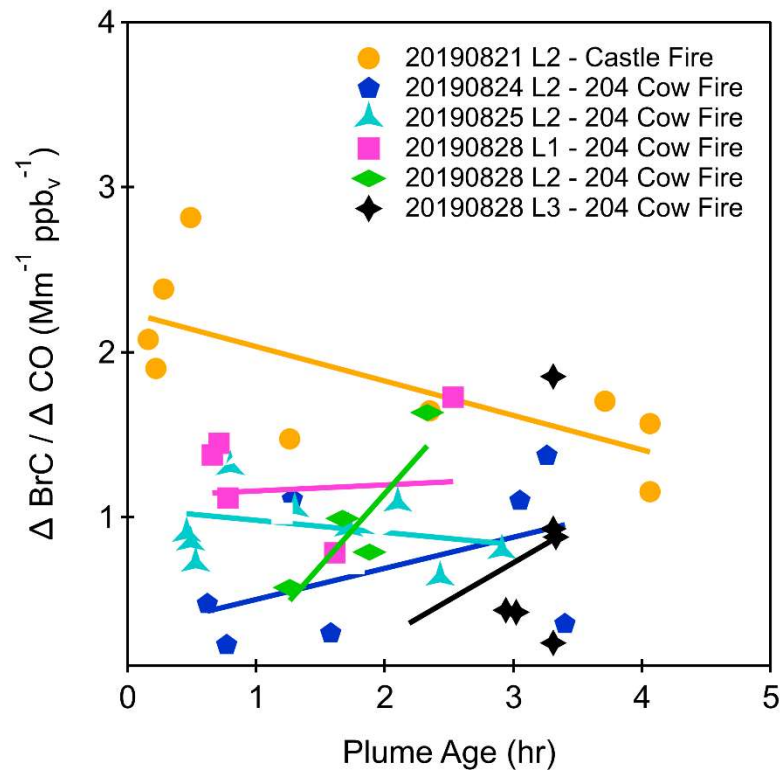
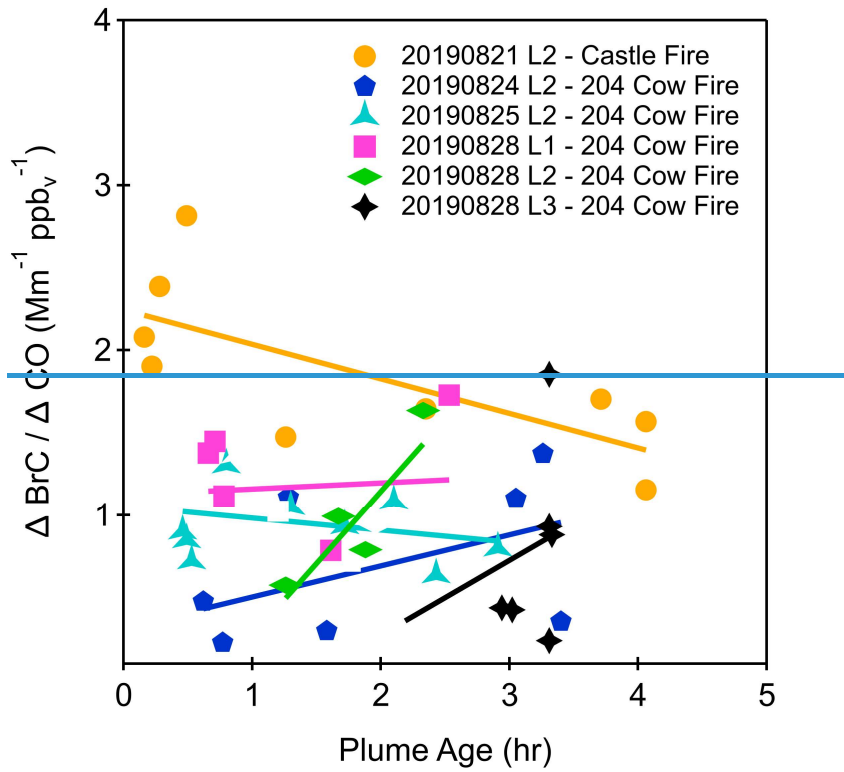
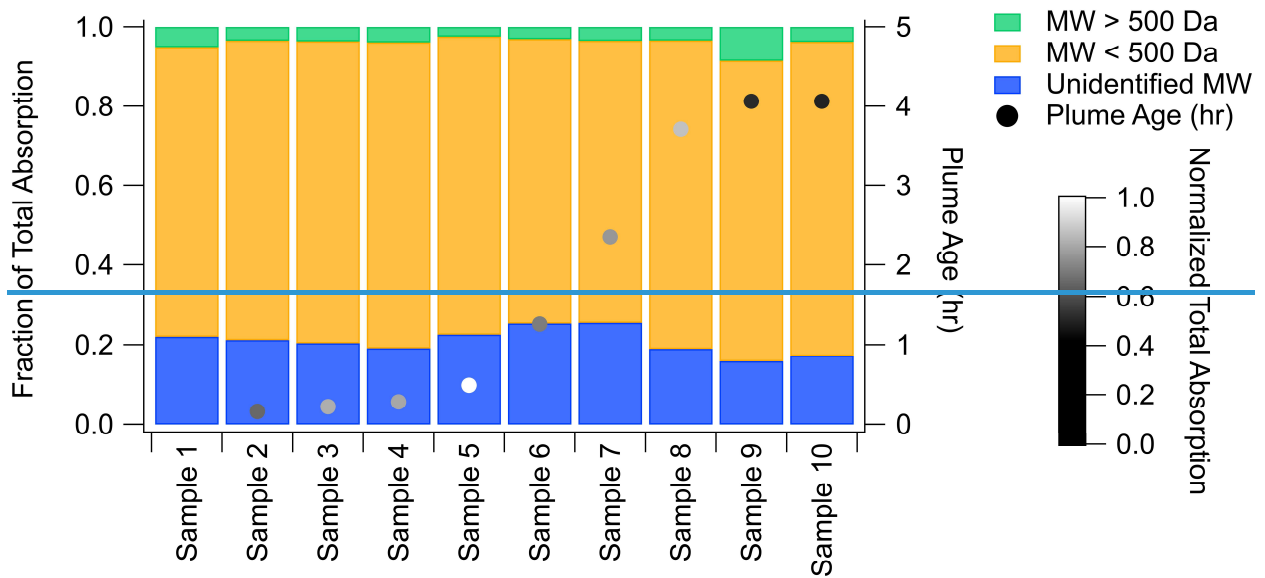


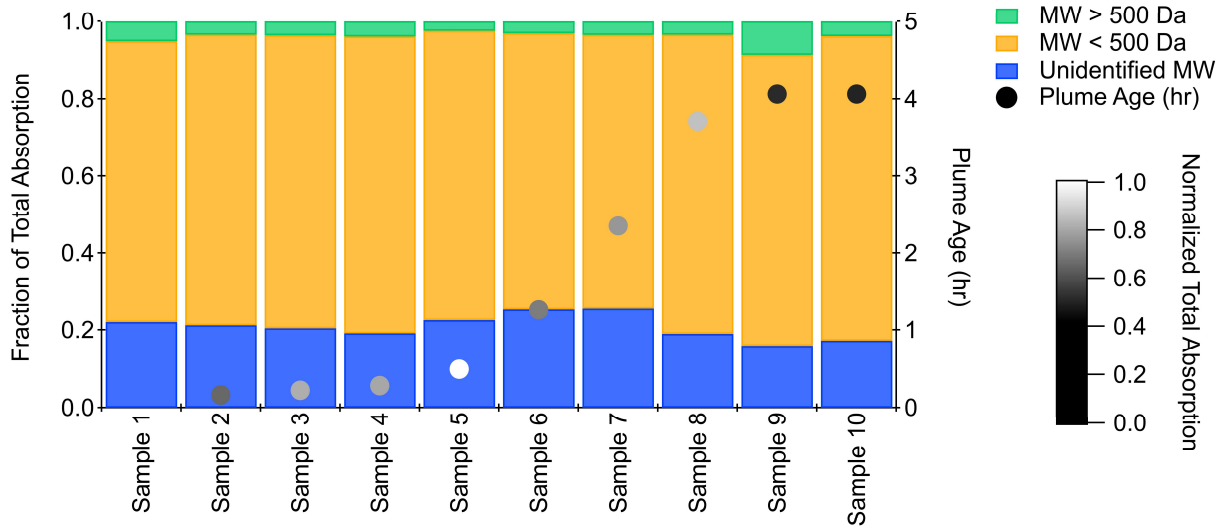
Figure 1.



833

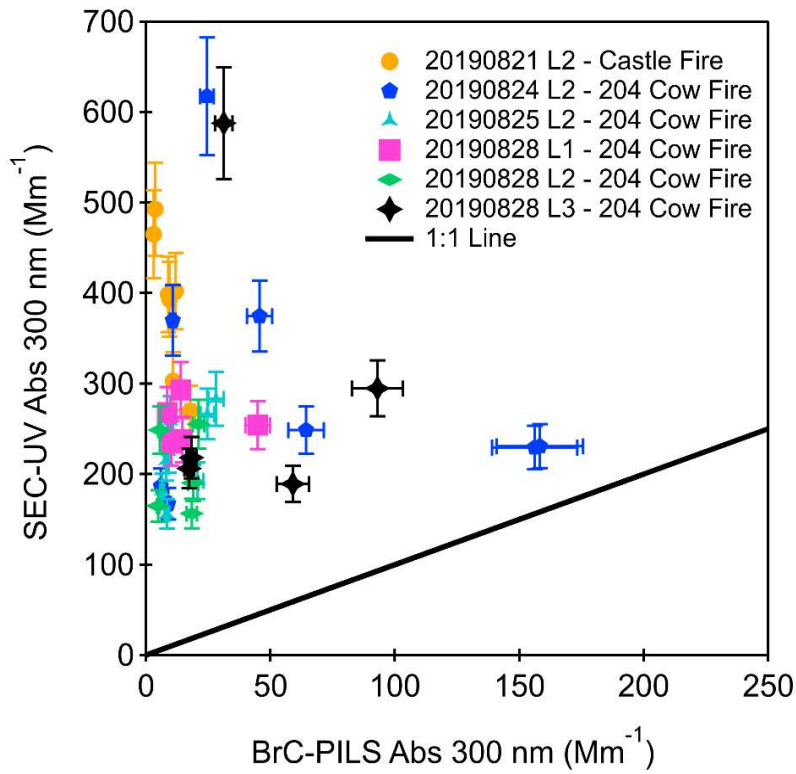
Figure 2.





836

Figure 3.



837

838

Figure 3.

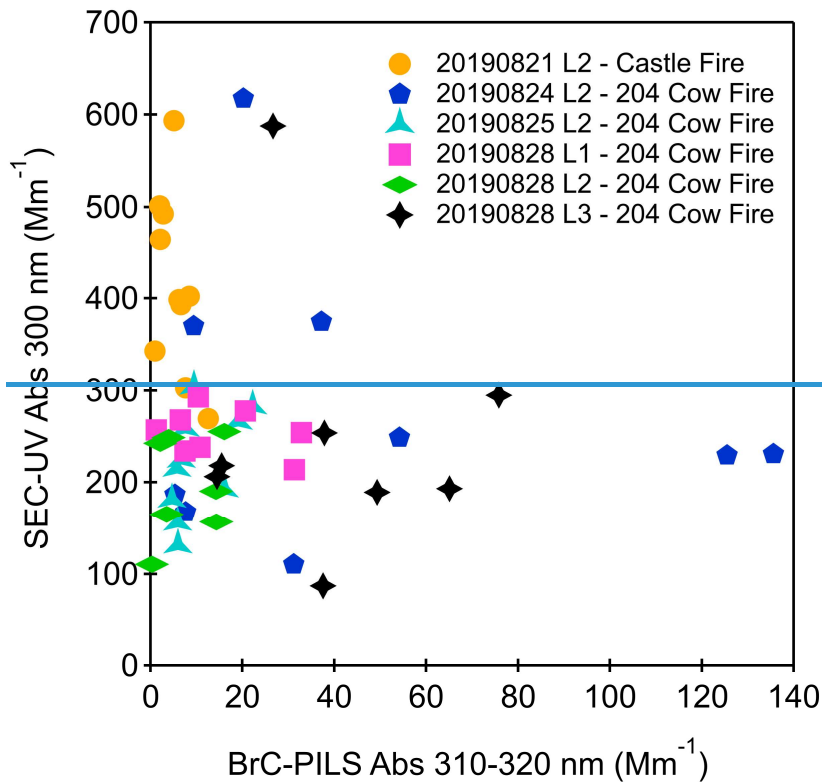


Figure 4.

